Adaptive control algorithm for improving power capture of wind turbines in turbulent winds

Diaz-Guerra, Lluis ; Adegas, Fabiano Daher; Stoustrup, Jakob; Monros, Miriam

Published in:
2012 American Control Conference (ACC)

Publication date:
2012

Document Version
Early version, also known as pre-print

Adaptive Control Algorithm for Improving Power Capture of Wind Turbines in Turbulent Winds

Lluís Díaz-Guerra, Fabiano Daher Adegas, Jakob Stoustrup and Miriam Monros

***Abstract*— The standard wind turbine (WT) control law modifies the torque applied to the generator as a quadratic function of the generator speed ($K\omega^2$) while blades are positioned at some optimal pitch angle (β^*). The value of K and β^* should be properly selected such that energy capture is increased. In practice, the complex and time-varying aerodynamics a WT face due to turbulent winds make their determination a hard task. The selected constant parameters may maximize energy for a particular, but not all, wind regime conditions. Adaptivity can modify the controller to increase power capture under variable wind conditions.**

This paper present new analysis tools and an adaptive control law to increase the energy captured by a wind turbine. Due to its simplicity, it can be easily added to existing industry-standard controllers. The effectiveness of the proposed algorithm is assessed by simulations on a high-fidelity aeroelastic code.

***Index Terms*— Wind Turbines, Adaptive Control, efficiency.**

I. Introduction

Automatic control of wind turbines is one of the engineering areas that received attention from both academia and industry during the last decade. A consensus from all the work done so far is that the wind turbine controller plays an important role on maximizing the energy generation while alleviating mechanical loads [1], [2], [3]. There are three main steps to develop a wind turbine controller: control objectives, control strategy and controller setup. The control objective is a qualitative and quantitative description of the goals which should be achieved by the controller such as energy capture, reduced dynamic mechanical loads and power quality. The other two subsequent steps are carried out to ensure that the controller objectives are satisfied. The control strategy is a selection of the operating points that the wind turbine should be regulated around. In the controller setup, controller structure is determined such as the controlled variables, the performance measures, the reference signals, the switching procedure between different controllers, as well as controller tuning.

Much of the research effort lies in the controller setup. Modern controllers of different structures - e.g. linear quadratic [4], linear parameter-varying [5], repetitive model predictive [6], to mention a few - were designed and their performance compared against traditional controllers. Despite the fact that modern controllers have in general better performance, the industry-standard controller for Region II remains the typical non-linear feedback law,

$$T_g = K\omega_g^2 \tag{1}$$

where T_g is the generator torque, ω_g is the generator speed, and K is a constant scalar. Blades are positioned at some optimal pitch angle β^*. The value of K and β^* should be properly determined to maximize energy capture; its poor selection can lead to significant energy loss. In practice, the complex and time-varying aerodynamics a wind turbine faces due to turbulent winds make the determination of these a hard task.

Techniques for improving the control strategy of a wind turbine are as important as the controller setup. In fact, to choose the values of K and β^* for increased energy capture has close relation to the proper selection of operating points. A maximum power strategy is the collection of operating points that maximizes the power coefficient (C_P) in steady-state. However, wind turbine operation does not move along the maximum C_P locus during transients. The aerodynamic stall front, which is close to the maximum C_P locus, is likely to be reached especially in turbulent winds and for rotors with "peaked" C_P surface. The operation on the stall region brings low conversion efficiency and ineffectiveness to rapidly restore operation to the desired operating locus due to dynamic wake and stall effects. Regulation at operating points with lower steady-state power capture is likely to result in higher energy capture when the turbulence intensity is considered [7], [8], [9], [10].

Adaptivity is interesting in this context because the controller can be modified to cope with the actual wind regime. Most adaptive algorithms to increase converted power are based on a "Hill-Climb" approach. Basically, the plant is excited and power performance evaluated. Small changes of the controller gain K is proposed in [9], [10]. Extremum seeking control algorithms [11], [12] excite the plant with sinusoidal signals, mainly rotational speed. Artificial intelligence like fuzzy logic [13] is used to infer the benefit of the excitation on power capture.

This paper presents a new analysis procedure and adaptive control law to increase the energy captured by a wind turbine. The result of the analysis is an alternative representation of the C_P surface, including the effects of the time-variability of tip-speed ratio on conversion efficiency. Instead of a hill-climb approach, the adaptive law utilizes the reformulated C_P information with online estimates of tip-speed ratio standard deviation to change the optimal controller gain and pitch angle accordingly. Simulations on a high-fidelity

L.D. Guerra is a MSc student in Automation Controls and Robotics at Polytechnic University of Catalonia (UPC), Barcelona, Spain. F.D. Adegas and Jakob Stoustrup is with the Dept. of Electronic Systems, Aalborg University, Denmark, fda@es.aau.dk.Miriam Monros is with ALSTOM - Ecotcnia, Spain.

aeroelastic code show the effectiveness of the proposed approach.

II. Adaptive Controller

A. Steady-State Power Conversion

In order to understand the proposed adaptive control law, the conversion of wind power into mechanical power in steady-state is explained here. The power that is captured from the wind field by an aerodynamic rotor can be represented by the following non-linear expression,

$$P_a = \frac{1}{2}\rho A C_P(\lambda,\beta)v^3, \tag{2}$$

where ρ is the air density, A is the rotor swept area, v is the effective wind speed, and C_P is the power coefficient of the aerodynamic rotor. Notice that the non-linearity comes from the dependence of C_P on the pitch angle β and on the tip-speed ratio λ,

$$\lambda = \frac{\omega R}{v}. \tag{3}$$

where R is the rotor radius and ω is the rotor angular speed. $C_P(\lambda,\beta)$ is a three-dimensional surface often computed by blade element momentum (BEM)-based aerodynamic codes.

The standard Region II controller (1) operates in the maximum power strategy when K is chosen as,

$$K = \frac{1}{2}\rho A R^3 \frac{C_P^*}{\lambda^{*3}}, \tag{4}$$

where λ^* is the optimal tip-speed ratio and β^* the optimal blade pitch angle that attains maximum power coefficient C_P^*. The NREL 5MW reference wind turbine [14] is used as the study case. The cut-in, rated, and cut-out wind speeds are 3 m/s, 11.4 m/s, 25 m/s, respectively. The C_P surface for this particular wind turbine is illustrated on Fig.1. Related optimal values are $C_P^* = 0.462$, $\lambda^* = 7.5$, $\beta^* = -0.3^o$, $K = 25.13\,\text{kNm/rpm}^2$.

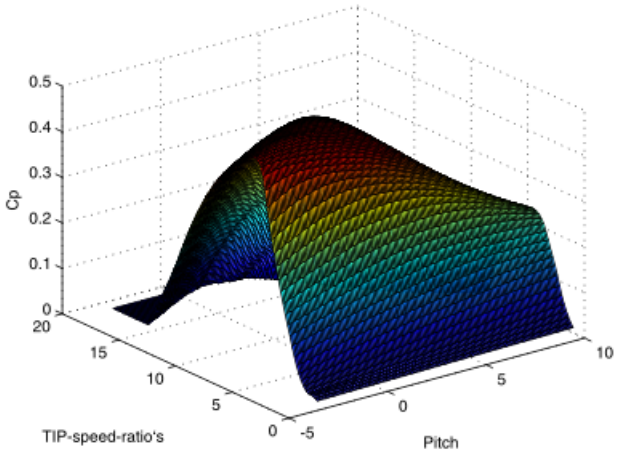

Fig. 1. NREL 5MW Power Coefficient (C_P) Curve

The $C_P(\lambda,\beta)$ and consequently λ^*, β^* are computed for steady-state wind speeds. However, the wind is turbulent and during transients the turbine does not move along the maximum C_P locus. A new method to analyze the energy captured of a turbulent wind is proposed next.

B. Turbulence Dependent Power Conversion

Due to the time-varying nature of the effective wind, it can be considered a normally distributed stochastic variable sampled over a finite time interval. Its sample standard deviation is given by,

$$\sigma_v = \sqrt{\frac{1}{N-1}\sum_{i=1}^{N}(v_i - \bar{v})^2}, \tag{5}$$

where v_i are the observed values of the sample items, $\bar{v}$ the mean value of all observed values and N is the number of observed values.

The finite time interval should be chosen in order to appropriately capture wind turbulence behavior. The time interval will also influence on how often the adaptive law updates the controller. According to [15], for local winds, wind turbulence spectrum has a peak at 50 cycles/h (1 min cycles) and presents high energy between thirty seconds and two minutes cycles. In this work, σ_v is computed with a time window of one minute.

The tip-speed ratio can be defined as time-varying due to its dependence on the wind speed,

$$\lambda_s(t) := \frac{\bar{\omega} R}{v(t)}. \tag{6}$$

Rotational speed is taken as a mean over a time window in (6), although in reality it varies in time. This simplification is convenient because the standard deviation of λ_s depends uniquely on the standard deviation of the wind speed,

$$\sigma_\lambda = f(\sigma_v), \tag{7}$$

and can be interpreted as how much the tip-speed varies due to wind turbulency for a mean rotational speed, during a time window. Thus, the probability density function of the tip-speed-ratio for a time window is

$$f(\lambda_s, \bar{\lambda}_s, \sigma_\lambda) = \frac{1}{\sqrt{2\pi\sigma_\lambda^2}}\exp\left(-\frac{(\lambda_s - \bar{\lambda}_s)^2}{2\sigma_\lambda^2}\right). \tag{8}$$

It is worth to highlight that instead of a deterministic variable like in the steady-state power conversion, λ_s is now a stochastic variable with normal probability density function (8). As a consequence, $C_P(\lambda_s,\beta)$ is also a stochastic variable. The C_P surface represented as a grid of points makes difficult its analytical representation as a stochastic variable. However, the convolution can be utilized to derive a modified version of the C_P surface that takes the stochastic variability into account. Recall that convolution is a mathematical operation on two functions g and h, producing a third function that is typically viewed as a modified version of one of the original functions. Taking $g := C_P(\lambda_s,\beta)$ and $h := f(\lambda_s, \bar{\lambda}_s, \sigma_\lambda)$,

$$C_P(\lambda_s,\beta) * f(\lambda_s, \bar{\lambda}_s, \sigma_\lambda) = \int_{-\infty}^{\infty} C_P(\tau,\beta) f(\lambda_s - \tau, \bar{\lambda}_s, \sigma_\lambda) d\tau \tag{9}$$

can be interpreted as a weighted average of the function $C_P(\tau, \beta)$ at the value λ where the weighting is given by $f(-\tau, \bar{\lambda}, \sigma_\lambda)$ simply shifted by amount λ. As λ changes, the weighting function emphasizes different parts of the input function. Figure 2 visually illustrates the convolution process.

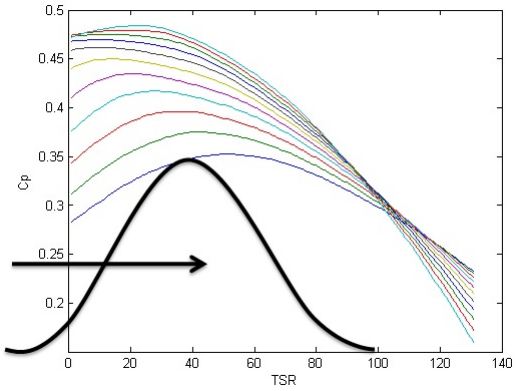

Fig. 2. Illustration of the convolution process.

Notice that the convolution can be taken for each fixed value of β. A three-dimensional modified $C_P(\lambda, \beta)$ surface is obtained when β is considered as variable in (9). From now on the modified surface is denoted stochastic power coefficient surface,

$$C_{Ps}(\lambda, \beta) := C_P(\lambda, \beta) * f(\lambda, \bar{\lambda}, \sigma_\lambda). \tag{10}$$

Stochastic power coefficient surfaces for different standard deviations can be seen in Fig. 3. From top-left to lower-right, $\sigma_\lambda = \{0.0, 1.0, 2.0, 3.0, 4.0, 4.8\}$. Notice that C^*_{Ps} is moved to higher λ values as σ_λ increases. A physical interpretation can be attributed to this behavior: when the wind turbulence increases, it is better to move the turbine to a "lightweight" mode. The generator torque should be reduced to give more freedom to the rotational speed to move like the wind speed does. This conclusion is in agreement with other references [7], [9]. A relation between the standard deviation σ_λ and the average λ that maximizes power capture is shown in Fig. 4.

The controller gain K differs if the λ^*_s and C^*_{Ps} are inserted in (11) instead of the steady-state ones. Notice that the value of K decreases for higher wind turbulences. The adapted controller gain is defined as

$$K_s := \frac{1}{2}\rho A R^3 \frac{C^*_{Ps}}{\lambda^{*3}_s}. \tag{11}$$

Another interesting observation is that C^*_{Ps} is attained for greater values of β as σ_λ increases. A relation can be found between optimal pitch angle β^*_s to maximize C_{Ps} and σ_λ as illustrated on Fig. 5.

Figure 6 shows a comparison between power coefficient values without any correction (green) and with correction (blue) on the optimal λ^* and β^*, for a turbulent wind speed

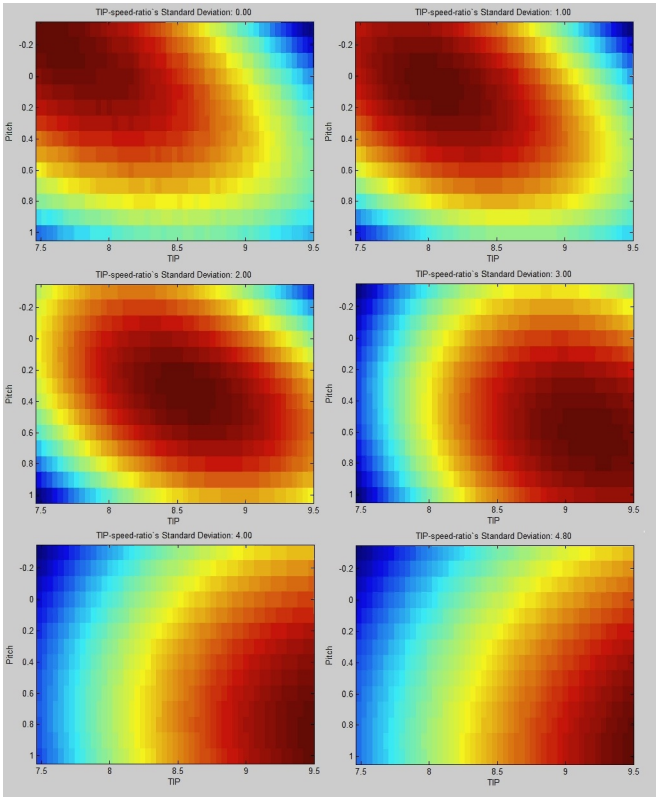

Fig. 3. Influence of TSR standard deviation on C_P Surface.

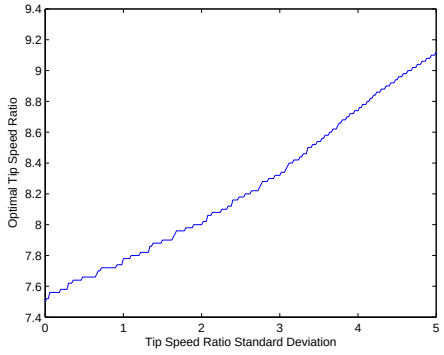

Fig. 4. Optimal λ^*_s for different σ_λ values.

of standard deviation σ_λ. As expected, for increased wind turbulence intensities, the difference is more prominent.

The before mentioned analysis is influenced by the shape of the steady-state C_P surface. Thus, resulting conclusions are dependent on each particular wind turbine. For example, peaked C_P surfaces may benefit more than wide surfaces.

C. Controller Structure

The analysis presented in the previous subsection suggests that both optimal λ^*_s and optimal β^*_s must be adapted online according to the increase on σ_λ in order to attain maximum conversion efficiency. It is not clear though how such adaptation can be implemented.

Figure 7 illustrates the adaptive controller structure. The

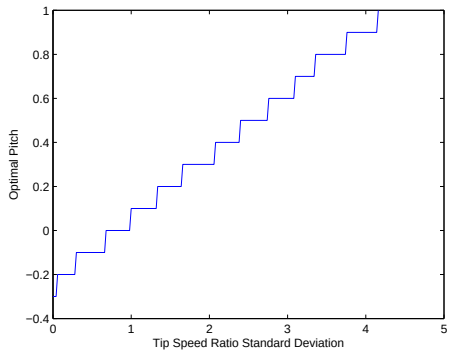

Fig. 5. Optimal β_s^* for different σ_λ values

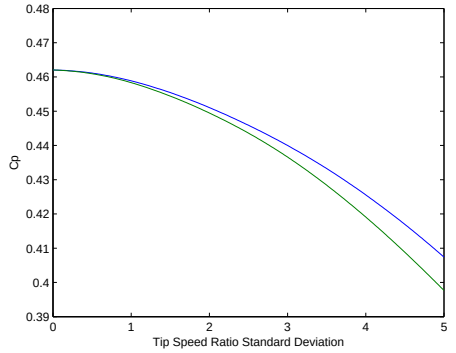

Fig. 6. Maximum C_P without (green) and with (blue) changes on λ^*, β^* at different σ_λ.

plant G (wind turbine) is regulated by the standard region 2 controller. The anemometer on the top of the nacelle is not a reliable indication of the wind speed. The effective wind speed $\widehat{v}$ driving the aerodynamic rotor is estimated by a wind speed estimator taking measurements of the generator torque T_g and rotational speed w. The tip-speed standard deviation σ_λ is computed from the estimated wind speed $\widehat{v}$ and the mean rotational speed $\bar{\omega}$ with a moving time window. The σ_λ is the input to look-up tables with optimal values of $\beta_s^*(\sigma_\lambda)$ and $K_s(\sigma_\lambda)$.

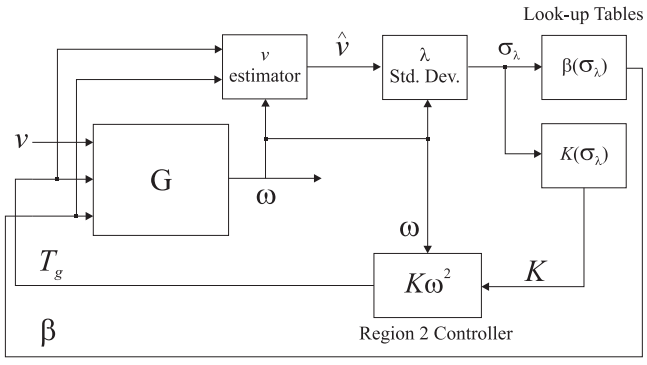

Fig. 7. Adaptive Controller Structure.

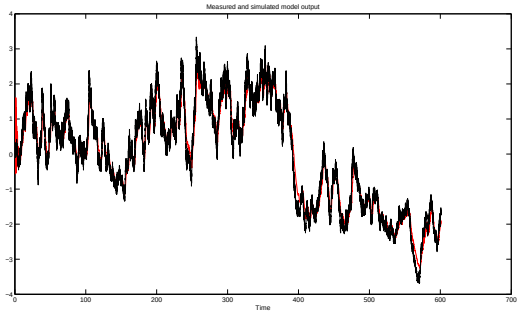

Fig. 8. Real Wind speed (Black) / Estimated Wind speed (Red)

D. Wind Speed Estimation

Here a simplified estimator is adopted because this work focus on Region 2 where non-linearities are not as prominent as in high wind speeds. A more elaborate wind speed estimator that encompasses all wind speed ranges can be found in [5].

The adopted wind estimator is a linear time-invariant transfer function relating signals ω and T_g to the estimated wind $\widehat{v}$,

$$\widehat{v} = \begin{bmatrix} G_{v,\omega} & G_{v,T_g} \end{bmatrix} \begin{bmatrix} \omega \\ T_g \end{bmatrix} \tag{12}$$

Each transfer function was obtained by MATLAB Identification toolbox® [17] applied to the time-series data generated by the aeroelastic code FAST ® [16]. The signals used in the identification process were the wind speed at hub height, rotational speed and generator torque. A normalized dataset was derived by removing the mean value of all signals. An ARX model was obtained using the identification toolbox with order selection facility. Time-series of the estimated wind speed compared with nonlinear simulation in FAST® is shown on Fig. 8. The comparison has a good agreement; a fit of 79.75% between the estimated and real wind values is achieved.

III. Simulation Results

Simulations in the aeroelastic code FAST with and without the adaptive controller shows the effectiveness of the proposed adaptation law. The simulation time length is 600 sec according to IEC61400 standard practices. Figure 9 brings time-series data of wind speed, controller gain K and pitch angle β for a wind speed with 40% turbulence intensity (TI).

Different wind conditions are simulated to evaluate controller performance. The stochastic wind characteristic is modeled by two distinct approaches, the first considering the wind as a normally distributed random process, and another as a Kaimal distribution, a more realistic wind model. A particular nomenclature labels the specific wind condition, for example:

- **8ND10:** $\bar{v} = 8m/s$, $\sigma_v = 10\%$, normally distributed.
- **8KS25:** $\bar{v} = 8m/s$; $\sigma_v = 25\%$, Kaimal distributed.

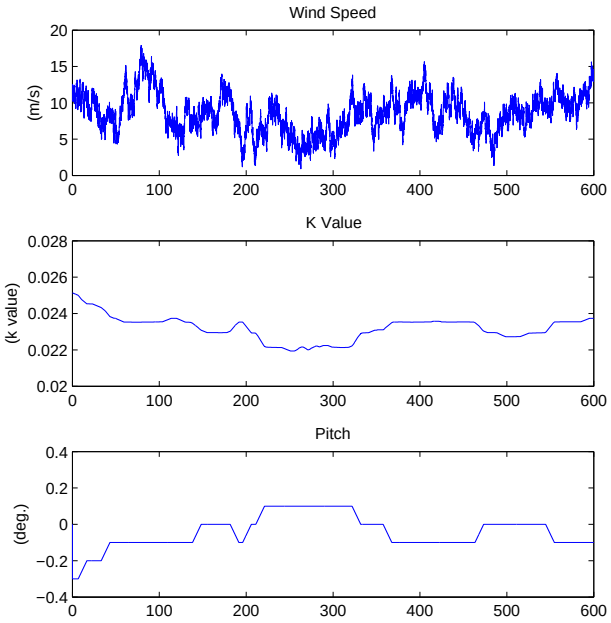

Fig. 9. Time-series for $8m/s$ mean and 40% turbulent wind speed.

TABLE I
AVERAGE POWER FOR NON-ADAPTIVE AND POWER INCREASE FOR ADAPTIVE CONTROLLERS

Wind	P_{avg} [MW]	ΔP_{avg} for $v(t)$ [%]	ΔP_{avg} for $\widehat{v}(t)$ [%]
8-00	1.79	0.00%	0.00%
8ND05	1.80	0.00%	0.01%
8ND10	1.42	0.07%	0.06%
8ND25	1.86	0.84%	0.43%
8KD05	1.74	0.00%	0.00%
8KD10	1.76	0.03%	0.03%
8KD25	1.91	0.21%	0.10%
8KD40	2.22	0.79%	0.41%
7KD05	1.18	0.01%	0.00%
7KD10	1.19	0.03%	0.03%
7KD25	1.29	0.20%	0.10%
7KD40	1.49	0.83%	0.47%

In the simulation for normal and Kaimal distributions, modified C_P tables calculated for a normal distribution were used.

The output power is averaged over the 600 sec to evaluate the increase on captured power. Table I shows the average power for the non-adaptive controller (P_{avg}) and the increase on average power (ΔP_{avg}) due to adaptivity, under different wind speed conditions. Adaptive controller is evaluated using the real wind speed signal on hub height v or the estimated wind speed signal $\widehat{v}$ to verify if wind speed estimation influences the results.

The adaptive controller increases the power captured for all wind speed conditions, with larger increase in higher turbulence intensities, as expected. Notice that the wind estimator has a negative impact on the captured power, suggesting that its low-pass filtering characteristic may influence the performance of the adaptive law, although a definitive conclusion cannot be drawn.

TABLE II
BLADES AND TOWER AVERAGE MOMENTS AT 8 M/S, 25% TI.

	For $v(t)$	For $\widehat{v}(t)$
Blade edgewise	0.04%	0.19%
Blade flapwise	0.29%	-0.45%
Tower side-to-side	-4.25%	-5.84%
Tower fore-aft	0.09%	0.02%
Tower torsional	3.09%	2.58%

The increase in power capture could lead to undesirable mechanical loads. Table II shows the percentage of average moment on various wind turbine components when compared to the standard controller.

Notice that mean tower and blade moments are slightly reduced except for the tower torsion. By looking at the averaged moments, the adaptive law does not have a negative impact on loads, but a definitive conclusion may only be drawn by comparing the equivalent damage of the components, which is not done on this work.

IV. CONCLUSIONS

This paper presents a new analysis procedure and an adaptive control law to increase the power captured by a wind turbine in turbulent winds. The result of the analysis procedure is a C_P surface considering the tip-speed ratio as a time-varying quantity. Such information is utilized in an adaptive control law to update the standard nonlinear torque-rotational speed relation and the optimal pitch angle according to the current wind turbulence. Due to its simplicity, the method can be easily augmented to a standard wind turbine control algorithm.

Simulations in a high fidelity aeroelastic code showed that wind turbine extracts more energy from the wind when the proposed analysis/adaptive controller is adopted. Apparently, the inclusion of adaptivity does not impact negatively the mechanical loads, although a definitive conclusion can only be drawn based on the equivalent damage of wind turbine components, not done in the present paper. A closed-loop stability analysis with time-varying controller gain is a subject of future work. Also planned for the future is a sensitivity study to investigate the assumption of fixed rotor speed in the time window that TSR is computed.

V. ACKNOWLEDGEMENTS

A special thanks to the reviewers, whose comments improved the quality of the manuscript.

REFERENCES

[1] Bossanyi, E.; *The Design of Closed Loop Controllers for Wind Turbines*. In: Wind Energy, Vol.3, pg. 149-163, 2000.
[2] Bossanyi, E., *Wind Turbine Control for Load Reduction*. In: Wind Energy, Vol. 6, pg. 229-244, 2003.
[3] Bossanyi, E., *Individual Blade Pitch Control for Load Reduction*. In: Wind Energy, Vol. 6, pg. 119-128, 2003.

[4] Ostergaard, K.Z.; Brath, P.; Stoustrup, J.; *Gain-scheduled linear quadratic control of wind turbines operating at high wind speed*. In: Proceedings of the 2007 IEEE Multi-conference on Systems and Control, Singapore, October 2007. IEEE.

[5] Ostergaard, K. Z. ; Stoustrup, J. ; Brath, P., *Linear parameter varying control of wind turbines covering both partial load and full load conditions*. In: International Journal of Robust and Nonlinear Control, Vol. 19, pg. 92-116, 2009.

[6] Friis, J.; Nielsen,E.; Bonding, J.; *Repetitive Individual Pitch Model Predictive Control for Horizontal Axis Wind Turbine*. Master thesis, Automation and Control, Aalborg University, 2010.

[7] Hansen, M., Hansen, A., Larsen, T., Oye, S., Sorensen, P., and Fuglsang, P. *Control design for a pitch-regulated, variable speed wind turbine*. Technical Report RISO-R-1500(EN), Riso National Laboratory, Denmark.

[8] Bianchi, F.D.; Mantz, R.J.; De Battista, H., *Wind Turbine Control Systems - Principles, Modelling and Gain Scheduling Design*. Springer-Verlag, 2007.

[9] Johnson, K.E. ; Fingersh, L.J.; Balas, M.J.; Pao, L.Y., *Methods for Increasing Region 2 Power Capture on a Variable Speed HAWT*National Renewable Energy Laboratory and University of Colorado, 2003

[10] Johnson, K.E. *Adaptive Torque Control of Variable Speed Wind Turbines*, National Renewable Energy Laboratory technical report NREL/TP-500-36265, 2003.

[11] Creaby, Justin.; Li, Y.; Seem, J. E.; *Maximizing Wind Turbine Energy Capture using Multivariable Extremum Seeking Control*. In: Wind Engineering, Vol. 33, No. 4, 2009.

[12] Munteanu, I.; Bratcu, A.I.; Ceanga, E.; *Wind turbulence used as searching signal for MPPT in variable-speed wind energy conversion systems*. In: Renewable Energy, Vol. 34, Issue 1, 2009, pg. 322-327.

[13] Simoes, M.G.; Bose, B.K.; Spiegel, R.J.; *Fuzzy Logic Based Intelligent Control of a Variable Speed Cage Machine Wind Generation System*. In: IEEE Trans. on Power Electronics, Vol. 12, No. 1, 1997.

[14] Jonkman, J. ; Butterfield, S. ; Musial, W. ; Scott, G. *Definition of a 5-MW Reference Wind Turbine for Offshore System Development*. NREL/TP-500-38060 technical report,National Renewable Energy Laboratory (NREL), 2009, USA.

[15] Van der Hoven, I., (1957). *Power spectrum of horizontal wind speed in the frequency range from 0.0007 to 900 cycles per hour.* J. Met., 14, 1604.

[16] NWTC Design Codes (FAST by Jason Jonkman, Ph.D.). http://wind.nrel.gov/designcodes/simulators/fast/

[17] MATLAB Software (Simulink and Identification Toolboxes)